Article

Multiplicative Renormalization of Stochastic Differential Equations for the Abelian Sandpile Model

Dimitri Volchenkov

Department of Mathematics and Statistics, Texas Tech University, 1108 Memorial Circle, Lubbock, TX 79409, USA; dimitri.volchenkov@ttu.edu

Abstract: The long-term, large-scale behavior in a problem of stochastic nonlinear dynamics corresponding to the Abelian sandpile model is studied with the use of the quantum-field theory renormalization group approach. We prove the multiplicative renormalization of the model including an infinite number of coupling parameters, calculate an infinite number of renormalization constants, identify a plane of fixed points in the infinite dimensional space of coupling parameters, discuss their stability and critical scaling in the model, and formulate a simple law relating the asymptotic size of an avalanche to a model exponent quantifying the time-scale separation between the slow energy injection and fast avalanche relaxation processes.

Keywords: self-organized criticality; multiplicative renormalization; critical scaling

1. Introduction

The *Abelian sandpile model* (ASM) was introduced by P. Bak, Ch. Tang, and K. Wiesenfeld [1] as an example of a cellular automaton following the Abelian dynamics [2] and displaying the *self-organized criticality* (SOC) property [3–9] that is considered to be the important mechanism contributing to complexity [4,10] in a way that could be linked to the critical phenomena theory [11,12]. Similarly to the scale-invariant systems being in a critical state, the SOC models do not possess characteristic scales, and the scaling exponents characterizing the power law asymptotes of Green functions are rather determined by the symmetries of interactions in these models [13,14]. However, unlike critical phenomena, the "critical states" in SOC models are the attractors of the automaton dynamics that are achieved without the tuning of any control parameters [15]. Criticality is characterized by the scale-invariant fluctuations referred to as a special state between order and chaos [16], and the self-tuning to criticality was reported in many disciplines as diverse as seismology [17,18], the percolation of gels [19], neuroscience [16,20–23], high-energy astrophysics [24,25], forest fires [26–28], sociology [29–31], data analysis [32], and the study of consciousness [33,34].

The effect of noise on the SOC dynamics was noticed a long time ago [35]. Although various models of noise lead to the same scaling exponents, the observed universality class is sensitive to noise, as the different assumptions about correlations of random forces injecting energy into the system give rise to different critical behavior [35]. Renormalization techniques [36] that are used to eliminate the singularities arising in long-term, large-scale asymptotic behaviors by altering the values of parameters and fields to compensate for the effects of their self-interactions seem to be an efficient approach to explore the problem in question. The critical state and the scale-invariant dynamics in sandpile models was studied with the use of a "real-space renormalization group" by introducing coarse-grained variables [37,38] and with a "dynamic renormalization group" by an elimination of the fast short-wave-length modes and the rescaling of the remaining modes in a truncated equation keeping a single cubic interaction term [39] as early as in 1994. Both approaches predicted a single attractive fixed-point, although their critical exponents differed. The

application of *renormalization group methods* (RGs) to SOC models was continued with varying conclusions in [40–43] just to mention a few manuscripts. The current state of discussion on the RG applications to SOC [44–47] may be accurately summarized by the following words excerpted from a title of one of the mentioned papers: "*dimensional transmutation and nonconventional scaling behavior*" in SOC.

In our work, we consider the original ASM [1]; formulate it as a problem of stochastic nonlinear dynamics following [39,41] whilst keeping all infinite numbers of interaction terms in the equation; prove the multiplicative renormalization of the model, including an infinite number of coupling parameters; calculate an infinite number of renormalization constants following the technique proposed in [48,49]; find a *plane of fixed points* in the infinite dimensional space of coupling parameters; discuss their stability and critical scaling in the model; and formulate a simple law relating the asymptotic size of an avalanche to a model exponent quantifying the time scale separation between the slow energy injection and fast avalanche relaxation processes in the ASM. The obtained law resembles the famous "*four-thirds*" phenomenological law of Richardson known in turbulent transport [50–52].

This paper is organized as follows. In Section 2, we formulated a stochastic differential equation for the ASM with the separation of the time scales related to energy injection and avalanche relaxation. In Section 3, we provided the functional integral formulation and introduced the Feynman diagram technique for the ASM. We proved that the related quantum-field theory is multiplicatively renormalizable and requires an infinite number of renormalization constants, each one corresponding to an individual term in the power series expansion describing nonlinear interaction in the model in Section 4. We demonstrated that all the terms in the power series expansion are equally important for UV renormalization (for the long-term, large-scale behavior), and therefore, the series cannot be truncated at any order of the expansion parameters, as was assumed beforehand [35,41]. In Section 5, we calculated an infinite number of renormalization constants in the one-loop order of diagram expansion, in the minimum subtraction scheme. Furthermore, in Section 6, we formulated the RG-equations for the ASM. The model allows for an entire two-dimensional plane of fixed points featured by two major expansion parameters in an infinite dimensional space of coupling constants associated with an infinite number of nonlinear interaction terms, as can be seen in Section 7. We also investigated the IR-stability of fixed points obtained at the previous step and conclude, in particular, that both energy injection assumptions on white noise and the "frozen" configuration of random forces that are particularly "popular" in the literature are IR-unstable, in a sense that the corresponding correlation functions do not have any stable long-term, large-scale asymptotes (Section 7). In Section 8, we discussed the critical scaling in the ASM corresponding to the different models of energy injection and calculated the asymptotic size of an avalanche. We conclude in the last section.

2. Stochastic Differential Equation for the ASM with the Time-Scale Separation between Energy Injection and Avalanche Relaxation

The microscopic rules of ASM are defined on a finite grid, $\mathcal{L} \subset \mathbb{Z}^d$, in which each site $i \in \mathcal{L}$ has an associated value that corresponds to the slope of the pile, usually called energy [53]. This slope builds up as "grains of sand" $\delta E > 0$ are randomly placed onto the pile until the local slope value exceeds a specific threshold value E_c at which time that site becomes active and collapses, transferring all energy (sand) to the adjacent sites, increasing their slope. The amount of energy perturbing the system is fixed at $\delta E = E_c/q$, where q is a coordination number, and the amount of energy transferred to neighbors from an active site is also fixed at E_c [1,14,41]. As a result, an avalanche that will affect many sites may emerge, as the neighboring sites can also be activated due to their energy further exceeding the threshold value E_c and transfer energy, until it is absorbed by the open boundary $E_{\partial \mathcal{L}}(t) = 0$, and all sites reached a value of energy smaller than E_c. The random placement of sand grains on the grid only resumes when the avalanche is terminated.

The ASM microscopic evolution rules can be written in the following form invariant under spatial translations, rotations, reflections, and parity transformation of the order parameter $E \rightarrow -E$ [14,41]:

$$E_i(t+1) - E_i(t) = \frac{E_c}{q} \sum_{j \sim i} \theta(E_j(t)) - \theta(E_i(t)) + \zeta_i(E, t), \tag{1}$$

in which $E_i(t)$ exceeds the energy over the critical value E_c. The external noise function, viz.,

$$\zeta_i(E, t) = \frac{E_c}{q} \delta_{i,\mathbf{n}(t)} \prod_{j \in \mathcal{L}} [1 - \theta(E_j(t))], \tag{2}$$

acts at a *slow time scale* when there are no active sites in the lattice. The random vector $\mathbf{n}(t)$ points at the site of random placement of sand grains $\delta E = E_c/q$. In comparison with the slow dynamics of random placements, and avalanches governed by the rules (1) evolve incomparably fast (as sand grains are added to the grid only after the avalanche is terminated) [14].

2.1. Stochastic Differential Equation for the Coarse-Grained ASM

For an appropriate choice of the lattice spacing a, the time step, and the coordination number q, the stochastic problem (1) and (2) is considered a coarse-grained version of the following stochastic differential equation for the scalar field $E(\mathbf{r}, t)$ [14,41]:

$$\frac{\partial E(\mathbf{r}, t)}{\partial t} = \mathfrak{A}_0 E_c \Delta \theta(E(\mathbf{r}, t)) + f(\mathbf{r}, t), \tag{3}$$

with a single dimensional parameter $\mathfrak{A}_0 > 0$, $[\mathfrak{A}] = L^2 T^{-1}$. The stochastic Equation (3) describes the diffusion of energy in $\mathbb{Z}^d$ issued from a source defined by $f(x)$, $x \equiv \mathbf{r}, t$. The function $f(x)$ in (3) is a sum of the multiplicative slow time scale *external noise* describing the energy injection into the system and the *internal noise* that appears due to the elimination of microscopic degrees of freedom and dissipation of energy at the lattice boundaries, as energy is pumped into the system when $f(x) > 0$ but disappears whenever $f(x) < 0$ [14]. In a stable sandpile configuration, $\langle f(x) \rangle = 0$, as both processes are balanced to correspond to an assumption of random boundaries defined on an infinite lattice with energy dissipation for each toppling site, instead of transferring it to neighbors.

The unit step function $\theta(E)$ in (3) is then regularized at zero, allowing for a power expansion with an infinite radius of convergence, viz.,

$$\theta(E) = \lim_{\Omega \to \infty} \frac{1 + \mathrm{erf}(\Omega E)}{2} \tag{4}$$

where $\mathrm{erf}(x) = \pi^{-1/2} \int_{-\infty}^{x} \exp[-y^2] \, dy$ is the error function, and Ω is a regularization parameter. Expanding the regularizing function (4) into the powers of E in (3), we obtain the following stochastic differential equation:

$$\frac{\partial E(\mathbf{r}, t)}{\partial t} = \mathfrak{A}_0 E_c \sum_{n \geq 1}^{\infty} \frac{v_{n0}}{n!} \Delta E^n(\mathbf{r}, t) + f(\mathbf{r}, t), \quad v_{n0} = \lim_{M \to \infty} M^n \theta^{(n)}(0), \quad n \in \mathbb{N} \tag{5}$$

where $\theta^{(n)}(0)$ is the $n-$th order derivative of the regularizing function (4) at zero. In (5), all even coupling constants vanish, as $\theta^{(2n+2)}(0) = 0$. Although $v_{n0} \to \infty$, as $M \to \infty$, the series in (5) converges. In the previous studies related to the renormalization of the ASM [41], the series in (5) was truncated at the third term, and then an attempt to study long-term, large-scale asymptotic behavior in a truncated model was made. However, the detailed analysis of UV-divergences in the integrals of the perturbation series and the multiplicative renormalization given in the forthcoming sections following [14] suggests

that all interaction terms $\mathfrak{A}_0 E_c \nu_{n0} \Delta E^n(\mathbf{r}, t)/n!$ are equally important, and therefore, none of them can be omitted.

In Equation (5) and throughout the paper, we shall mark the bare, unrenormalized parameter $\mathfrak{A}_0$ and the coupling constants ν_{n0} with the "0"-index to distinguish them from their renormalized analogs, which we shall denote in forthcoming sections as $\mathfrak{A}$ and ν_n, respectively. In what follows, we include the threshold value E_c into the coupling constants ν_{n0} to simplify the notation.

2.2. Co-Variance of Random Forces with Time-Scale Separation

While, in the slow time scale of energy injection, the random dynamics can be taken into account as white noise $F(x)$, $x \equiv \mathbf{r}, t$ [14], viz.,

$$\langle F(x) \rangle = 0, \quad D_F \equiv \langle F(x)F(x') \rangle = 2\Gamma \delta^d(\mathbf{r} - \mathbf{r}')\delta(t - t') \tag{6}$$

where Γ is the Onsager coefficient, the fast time scale dynamics of avalanche relaxation can be modeled by the linear Langevin equation driven by the slow time-scale white noise $F(x)$ [14], viz.,

$$\frac{\partial f(x)}{\partial t} + \mathfrak{R}f(x) = F(x), \quad \mathfrak{R}(k) \equiv \varrho_0 \mathfrak{A}_0 k^{2-2\kappa}. \tag{7}$$

Without loss of generality, we assume in (7) that the anomalous diffusion can be described in Fourier space by a pseudo-differential operator $\mathfrak{R}$ characterized by the exponent $2\kappa > 0$ and the coupling constant $\varrho_0 > 0$ related to the reciprocal correlation time $t_c(k) = k^{2\kappa-2}/\varrho_0 \mathfrak{A}_0$ at wave number k [14]. As usual, the "0"-index denotes the bare, unrenormalized values of the parameters. The unrenormalized coupling constant ϱ_0 corresponds to the microscopic degrees of freedom omitted from Equation (3) in the course of the coarse-graining of the microscopic rules (1), and therefore, it is related to the UV momentum scale (of energy injection) as $\varrho_0 \simeq \Lambda^{2\kappa}$ [14]. The coefficient of anomalous diffusion $2 - 2\kappa$ is related by $\kappa = d/2(1 - \tau)$ to the Lyapunov spectrum with a universal exponent $\tau < 1$ describing the energy transport in the lattice [8].

The covariance of the slow time scale random force (6) is modeled in Fourier space by the following power law asymptotics at large k:

$$\langle F(\mathbf{k}, \omega)F(-\mathbf{k}, \omega') \rangle \equiv D_F(k) \propto \varrho_0 \mathfrak{A}_0^3 k^{6-d-2\epsilon-2\kappa}. \tag{8}$$

The physical dimension $[\langle FF \rangle] = L^d T^{-3}$ is built in the power law model (8) from $\mathfrak{A}_0$ and k, which is the only dimensional parameter in the problem. However, the white noise assumption (6) requires that D_F should be constant in Fourier space, and therefore, we need a regularization parameter $\epsilon > 0$ quantifying the departure of the physical model from the logarithmic theory (when $\epsilon = 0$), similarly to the well-known $\varepsilon = 4 - d$ expansion parameter in the critical phenomena theory [11,13,14], although 2ϵ in the model (8) is *not* related to the space dimension d. Finally, although the spectral density of the energy injection is independent of the correlation time $t_c(k)$ at any given wave number k, the slow time scale random force covariance (8) should be proportional to a dimensionless coupling constant $\varrho_0 k^{-2\kappa}$, which is a small formal parameter of the perturbation theory [14]. The exponents 2κ and 2ϵ in (8) are the parameters of double expansion in the $\{\kappa - \epsilon\}$ plane around the origin $\kappa = \epsilon = 0$, with the additional convention that $\epsilon = O(\kappa)$, and their physical values are taken such that $6 - d = 2(\kappa + \epsilon)$, for the case of random force uncorrelated in space, $D_F(k) \propto \text{Const}$ [14].

Then, it follows from (7) that the covariance of the fast time-scale random force f should be consistent with the model (8) [14], viz.,

$$D_f(\omega, k) = \frac{D_F(k)}{\omega^2 + [\varrho_0 \mathfrak{A}_0 k^{2-2\kappa}]^2} \propto \frac{\varrho_0 \mathfrak{A}_0^3 k^{6-d-2\epsilon-2\kappa}}{\omega^2 + [\varrho_0 \mathfrak{A}_0 k^{2-2\kappa}]^2}. \tag{9}$$

The model (9) has a formal resemblance with the models of random walks in a random environment under long-range correlations. On the one hand, in the rapid-change limit $\varrho_0 \to \infty$, the covariance model (9) takes the form $D_f(\omega, k) \to \mathfrak{A}_0 k^{2-d-2\epsilon+2\kappa}/\varrho_0$ that reduces to the uncorrelated white noise model (6) with $\Gamma = \mathfrak{A}_0/2\varrho_0$ for $\epsilon - \kappa = 1 - d/2$. On the other hand, in the limit of "frozen" configuration, $\varrho_0 \to 0$, the external random force acts continuously in time, and the covariance (6) is static, viz., $D_f(\omega, k) \to \pi\varrho_0 \mathfrak{A}_0^2 k^{4-d-\epsilon}\delta(\omega)$.

3. Functional Integral Formulation and Feynman Diagram Technique for the ASM

A stochastic dynamics problem is equivalent to a quantum field theory of the doubled set of fields, E and E' (each basic field acquires an auxiliary field) [13,14,54–56], in the sense that the statistical averages $\langle\ldots\rangle$ of the dynamic quantities over the ensemble of configurations in the stochastic problem can be identified with the functional averages taken with weight $\exp S(E, E')$ for some action functional $S(E, E')$. The generating functional of full Green functions for the stochastic problem (5) can be represented by the following functional integral [14]:

$$G(A) = \int \mathcal{D}E\, \mathcal{D}E'\, \exp\left[S(E, E') + \int dx\, \left(A_E(x)E(x) + A_{E'}(x)E'(x) \right) \right] \tag{10}$$

with the action functional

$$S(E, E') = \frac{1}{2} \int dx \int dx'\, E'(x)D_f(x, x')E'(x') + \int dx\, E'(x)\left[-\partial_t E(x) + \mathfrak{A}_0 \sum_{n\geq 1}^{\infty} \frac{\nu_{n0}}{n!} \Delta E^n(x) \right] \tag{11}$$

where $x \equiv \mathbf{r}, t$, and the arbitrary sources $A_E(x)$ and $A_{E'}(x)$ can be interpreted as the non-random external forces, so that the Green function $\langle E(x)E'(x')\rangle$ of the model (11) coincides with the simplest response function $\langle \delta E(x)/\delta f(x')\rangle$ of the original stochastic problem (5). All possible boundary conditions and the trivial asymptotic conditions for the fields $E(x)$ and $E'(x)$ at infinity are included in the domain of the functional integration $\mathcal{D}E\, \mathcal{D}E'$ over E and E' [14].

The standard Feynman diagram representations for the functional integral (10) are common to all models of stochastic nonlinear dynamics [13,14,54] and comprise the directed lines corresponding to the delayed ($\overleftarrow{\Delta}$) and advanced ($\overrightarrow{\Delta}$) propagators, viz.,

$$\overleftarrow{\Delta} \equiv< EE' >_0 = (-i\omega + \mathfrak{A}_0\nu_{10}k^2)^{-1}, \quad \overrightarrow{\Delta} \equiv< E'E >_0 = < EE' >_0^*, \tag{12}$$

and the undirected line corresponding to the pairwise propagator of the major field E, viz., $\Delta \equiv< EE >_0 = \overleftarrow{\Delta} D_f(k, \omega) \overrightarrow{\Delta}$. The pairwise propagator of the auxiliary field E', $< E'E' >_0 = 0$. In the diagrammatic expansion, there is an *infinite* number of $(n+1)$-leg interaction vertices $E'\Delta E^n$ proportional to the factors $\mathfrak{A}_0\nu_{n0}/n!$ playing the role of expansion parameters. In Fourier space, these interactions are $\propto k^2$, that is, they factored out to each external line E' in the Feynman diagrams, reducing the degree of UV superficial divergences in the 1-irreducible Green's functions [14]. Furthermore, as the delayed and advanced propagators (12) in the time representation are proportional to the unit step function $\theta(t - t')$, all diagrams for the 1-irreducible Green functions (without E'), all vacuum loops, as well as all connected functions $< E'\ldots E' >$ (without E) vanish identically, because of their diagrams contain the closed cycles of delayed propagators. We also assume that $\theta(0) = 0$, so that the self-contracted lines $\mathrm{Tr}[\overleftarrow{\Delta}]$ and $\mathrm{Tr}[\overrightarrow{\Delta}]$ vanish, and all Feynman graphs that do not arise in the iterations of the perturbation theory.

Correlation functions $\langle E(x_1)\ldots E(x_k)\rangle$, $x \equiv \mathbf{r}, t$ of the field $E(x)$ and response functions $\langle \delta^m[E(x_1)\ldots E(x_k)]/\delta f(x'_1)\ldots \delta f(x'_m)\rangle$ expressing the system response to an external perturbation are represented by the infinite sums of Feynman-like graphs with n-line vertices and two types of lines, Δ and $\overleftarrow{\Delta}$ [14]. In Figure 1, we drew the one-loop order

diagram expansions for the pairwise correlation function $\langle EE \rangle$ (as can be seen in Figure 1a) and the simplest response function $\langle \delta E / \delta f \rangle$ (see Figure 1b).

(a)

(b)
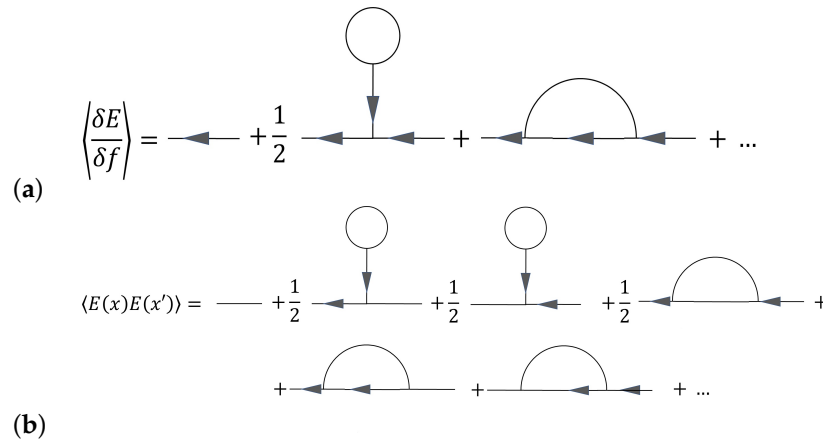
Figure 1. The one-loop order diagram expansions for the simplest response function $\langle \delta E / \delta f \rangle$ and the pairwise correlation function $\langle EE \rangle$.

The diagram expansions shown in Figure 1 are typical for the stochastic nonlinear dynamics problems [12–14,54–56]. In particular, the first graphs of the diagram expansions (presented in Figure 1) coincide with the Wyld diagrams obtained for the stochastic Navier–Stokes equation in the theory of fully developed turbulence [57], although they differ in the orders with two or more loops [14].

The diagram expansions like those shown in Figure 1 are stable if small perturbations decay with time, i.e., the singularities of diagrams in the frequency domain ω lie in the lower half-plane of the complex plain. For the bare response functions, stability is ensured by the correct sign of the $\mathfrak{A}_0 k^2 > 0$ [14]. The exact response function given by the Dyson equation, viz.,

$$< EE' > = \left[-i\omega + \mathfrak{A}_0 \nu_{10} k^2 - \Sigma_{EE'}(\omega, k) \right]^{-1}, \tag{13}$$

where $\Sigma_{EE'}(\omega, k)$ is an infinite sum of 1-irreducible graphs of the diagram expansion [14]. In the one-loop order (shown in Figure 1a), the only 1-irreducible diagram corresponds to

$$< EE' > \simeq_{1-\text{loop}} - \int \frac{d\omega'}{2\pi} \int \frac{d\mathbf{p}}{(2\pi)^d} \frac{\Delta(\omega', p)}{-i(\omega + \omega') + \mathfrak{A}_0 \nu_{10}(\mathbf{p} + \mathbf{k})}, \tag{14}$$

where $p \equiv |\mathbf{p}|$, and the bare propagator $\Delta(\omega, k) \equiv < EE >_0$ in the $(k, \omega)-$representation has the form [14]

$$\Delta(\omega, k) = \frac{\varrho_0 \mathfrak{A}_0^3 k^{6-d-2\epsilon-2\kappa}}{\left(\omega^2 + [\varrho_0 \mathfrak{A}_0 k^{2-2\kappa}]^2 \right) \left(\omega^2 + \mathfrak{A}_0^2 \nu_{10}^2 k^4 \right)}. \tag{15}$$

Integrating (14) over ω' results in

$$< EE' > \simeq_{1-\text{loop}} - \frac{\mathfrak{A}_0^2}{2\varrho_0} \int \frac{d\mathbf{p}}{(2\pi)^d} \frac{p^{2-d-2\epsilon}}{-i\omega + \mathfrak{A}_0 \nu_{10}(\mathbf{p} + \mathbf{k})^2 + \varrho_0 \mathfrak{A}_0 k^{2-2\kappa}}. \tag{16}$$

Within the order of perturbation theory, the self-energy term $\Sigma_{EE'}$ is proportional to the small parameter $\propto \varrho_0^{-1}$ and therefore cannot compete with the bare contributions $\propto \mathfrak{A}_0 \nu_{10} k^2$ [14]. However, if the integral (14) diverges as $k, \omega \to 0$, the IR-singularities would compensate the smallness of the coupling constant, so that the entire series $\Sigma_{EE'}$ should be summed to ensure the diagram expansion validity. The integral (14) is IR-divergent if either $\kappa < 0$, $\epsilon > 0$ or $\kappa > 0$, $\epsilon > \kappa$. For the rest of the $(\epsilon - \kappa)$-plane, the leading term governing the long-term, large-scale asymptotic behavior is trivial since it is

dominated by the bare contribution $\propto \mathfrak{A}_0 \nu_{10} k^2$, while other contributions $\propto \nu_{n0}$, $n > 1$ are negligible [14].

The strength of IR-singularities in the diagrams increases with the number of loops and decreases for small ϵ and κ, vanishing at $\epsilon = \kappa = 0$, i.e., at a logarithmic point corresponding to the interaction-free and linearized problem. However, we cannot set $\epsilon = \kappa = 0$, because of the UV divergence of the integrals at this point. Diagrams in $\Sigma_{EE'}$ are UV-divergent when $\kappa > 0$, $\epsilon < 0$ and $\kappa < 0$, $\epsilon < \kappa$, and therefore require a UV- cutoff at $k \simeq \Lambda$. The elimination of these singularities from all diagrams is performed by the standard procedure of UV-renormalization [13,14,36].

4. Multiplicative UV-Renormalization of the ASM

The analysis of UV-divergences in diagram expansion for the ASM is based on the dimensional counting arguments [13,14,36,54] applied to the action functional (11)—each term in that should be "dimensionless" with respect to the scaling transformations of space and time.

Theorem 1. *The Abelian sandpile model is multiplicatively renormalizable with a countably infinite number of renormalization constants.*

Proof of Theorem 1. With respect to the scaling transformations of momentum and frequency, any quantity Q in the problem in question is characterized by $d^k[Q]$ and $d^\omega[Q]$, the relevant momentum and frequency *canonical* dimensions, respectively. Assuming that $d^k[k] = d^\omega[\omega] = 1$, $d^k[\omega] = d^\omega[k] = 0$ and noting that $\omega \sim k^2$ (as $\partial_t \sim \Delta$ in the linearized equation of the model), one can introduce a *total* canonical dimension of a quantity Q as $d[Q] = d^k[Q] + 2d^\omega[Q]$ in the model [14]. In particular, $d[k] = d^k[k] + 2d^\omega[k] = 1$, and $d[\omega] = d^k[\omega] + 2d^\omega[\omega] = 2$. The canonical dimensions of the fields and parameters in the ASM are given in Table 1 and (adopted from [14]). As usual, the unrenormalized values of parameters are denoted in Table 1 by the "0"-index.

Table 1. Canonical dimensions of the fields and parameters in the ASM.

Q	E	E'	ν_{n0}	ν_n, ϱ	$\mathfrak{A}, \mathfrak{A}_0$	ϱ_0
d^k	$-\epsilon$	$d + \epsilon$	$(n-1)\epsilon$	0	-2	2κ
d^ω	0	0	0	0	1	0
d	$-\epsilon$	$d + \epsilon$	$(n-1)\epsilon$	0	0	2κ

Due to the nonlinear interactions in the model apart from the logarithmic point, the canonical dimension of the frequency $d[\omega]$ is replaced in the long-term and large-scale asymptotes with a *critical* dimension of frequency, $\Delta[\omega] = 2 + \gamma_\omega$, in which γ_ω is some *anomalous* dimension of frequency [13,14,54]. Similarly, apart from the logarithmic point, the canonical dimension of a quantity $d[Q]$ changes in the long term and large-scale asymptotes to the corresponding *critical* dimension [14], viz.,

$$\Delta[Q] = d^k[Q] + \Delta[\omega] \cdot d^\omega[Q] + \gamma_Q, \tag{17}$$

where γ_ω is some *anomalous* dimension of Q. The formal degree of UV divergence of a correlation function G comprising N_E fields E and $N_{E'}$ fields E' is given by the following divergence index [13,14,54]:

$$\delta_G = d + 2 - \left(N_E d[E] + N_{E'} d[E'] \right) \tag{18}$$

where d is the dimension of space. All diagrams (integrals) contributing to the same correlation function are characterized by the same divergence index (18). The diagrams correspond to the divergent integrals and therefore require compensating counter-terms in the course of UV-renormalization present in the correlation functions G, for which δ_G is a non-negative integer [13,14,54]. As we have already mentioned, all correlation

functions that only contain the major fields E (without E') vanish and, consequently, do not require counter-terms [13,14,54]. It is also important to mention that the actual degree of divergence δ'_G may be smaller than the formal divergence degree δ_G defined in (18) if the correlation function G contains derivatives that can be factored out of the diagram loop integral onto the external E'-field [14]. For example, the Laplace operator Δ can be moved onto the field E' by the integration by parts in the diagrams for each interaction vertex $E'\Delta E^n$, so that $\delta'_G = (d+2)(1-N_{E'})$, although $\delta = (1-N_{E'})d+2$. We conclude that, for any space dimension d, the superficial (logarithmic) UV divergences can only exist in the 1-irreducible diagrams corresponding to the functions $< E'E \ldots E >$ comprising a single auxiliary E' field ($N_{E'} = 1$) and an arbitrary number N_E of the major field E, for which $\delta_{<E'E...E>} = 2$, but $\delta'_{<E'E...E>} = 0$, and therefore all relevant counter-terms must have the form $E'\Delta E^n$ [14].

The inclusion of required counter-terms compensating the superficial (logarithmic) UV divergences in the model is reproduced by the multiplicative renormalization of the bare parameters $\mathfrak{A}_0$, ϱ_0, ν_{n0} and fields E, E' as follows [14]:

$$\mathfrak{A}_0 = \mathfrak{A}Z_{\mathfrak{A}}, \quad \varrho_0 = \varrho\mu^{2\kappa}Z_{\varrho}, \quad \nu_{n0} = \nu_n\mu^{(n-1)\epsilon}Z_{\nu_n}, \quad E = E_R Z_E, \quad E' = E'_R Z_{E'} \quad (19)$$

where μ is the renormalization mass parameter ($d^k[\mu] = 1$, $d^{\omega}[\mu] = 0$, $d[\mu] = 1$) expressing the non-uniqueness of the UV-renormalization procedure, E_R and E'_R are the renormalized analogs of the fields E and E', and Z_Q are the particular renormalization constants of the corresponding quantities Q. As all the terms of the renormalized action functional are dimensionless with respect to the scaling transformations of space and time, the particular renormalization constants should be related to each other as follows: $Z_E = Z_{\mathfrak{A}}$, $Z_{E'} = Z_{\varrho} = Z_{\mathfrak{A}}^{-1}$, and the renormalized action functional free of the UV-divergences takes the following form [14]:

$$S(E_R, E'_R) = \frac{1}{2}\int dx \int dx'\, E'_R(x)D_f(x,x')E'_R(x') + \int dx\, E'_R(x)\left[-\partial_t E_R(x) + \mathfrak{A}\sum_{n\geq 1}^{\infty}\frac{Z_n\mu^{(n-1)\epsilon}\nu_n}{n!}\Delta E_R^n(x)\right], \quad (20)$$

in which the renormalization constants $Z_n \equiv Z_E^n Z_{\nu_n} = Z_{\mathfrak{A}}^n Z_{\nu_n}$ that are directly calculated from the diagrams of perturbation theory expansion. □

5. Calculation of an Infinite Number of Renormalization Constants in the ASM

Following [14], we calculate an infinite number of the renormalization constants Z_n in the one-loop approximation in the minimal subtraction scheme using the method developed in relation to the problem of turbulent convection of a passive scalar impurity and the problem of growing phase boundary [48,49].

Theorem 2. *In the minimal subtraction scheme, in which only the poles are subtracted from the divergent integrals, in the one-loop approximation, the renormalization constants Z_n have the following form:*

$$Z_n = 1 - \frac{1}{2^{d-1}\pi^{d/2}\Gamma(d/2)}\sum_{\ell=0}^{\infty}(-1)^{\ell}\frac{\varrho^{2\ell}}{\nu_n}\sum_{m=0}^{n}\left(X_{mn}\frac{\ell^m}{2\epsilon+4\kappa\ell} + Y_{mn}\frac{\varrho\ell^m}{2\epsilon+2\kappa(2\ell+1)}\right) \quad (21)$$

where X_{mn} and Y_{mn} are the polynomials of the variables ν_k/ν_1, $k \leq n$.

Proof of Theorem 2. The generating functional of 1-irreducible Green functions $\Gamma(\mathcal{E})$, $\mathcal{E} \equiv \{E, E'\}$ of the field theory (11) is defined by the Legendre transform of the connected Green functions $W(A)$ (10) with respect to the source fields $A_{\mathcal{E}}(x)$ [14], viz.,

$$\Gamma(\mathcal{E}) = W(A_{\mathcal{E}}) - \sum_{\mathcal{E}}\int dx[A_{\mathcal{E}}(x)\mathcal{E}(x)], \quad \mathcal{E} \equiv E, E'. \quad (22)$$

The one-loop order contribution $\Gamma^{(1)}(\mathcal{E})$ to (22) is given by [14]

$$\Gamma^{(1)}(\mathcal{E}) = -\frac{1}{2}\mathrm{Tr}\,\log\left(K_{\mathcal{E}\mathcal{E}}K_0^{-1}\right),\quad K_{\mathcal{E}\mathcal{E}} \equiv \begin{pmatrix} K_{EE} & K_{EE'} \\ K_{E'E} & K_{E'E'} \end{pmatrix},\quad K_0 \equiv \begin{pmatrix} 0 & \overset{\leftarrow}{\Delta} \\ \overset{\rightarrow}{\Delta} & \Delta \end{pmatrix} \tag{23}$$

where

$$K_{EE} = -\mathfrak{A}\sum_{n>1}\frac{\nu_n\mu^{(n-1)\epsilon}}{(n-2)!}E^{(n-2)}\,\Delta E',\quad K_{EE'} = -\partial_t - \mathfrak{A}\sum_{n\geq 1}\frac{\nu_n\mu^{(n-1)\epsilon}}{(n-1)!}E^{(n-1)}\,\Delta, \tag{24}$$

$$K_{E'E'} = -D_f,\quad K_{E'E} = K_{EE'}^\top. \tag{25}$$

We are interested in the linear terms in the auxiliary field $E'(x)$ only, as others do not diverge. Moreover, we can consider the functions $\Delta E'(x)$ and $E(x)$ to be constants, neglecting their inhomogeneity in x, as the actual UV-divergence degree is $\delta' = 0$, and therefore, we need estimations for divergent parts at zero external momenta, $k = 0$. Using the relation $\delta(\mathrm{Tr}\log K) = \mathrm{Tr}(K^{-1}\delta K)$, we obtain the following expression for the one-loop order contribution [14]:

$$\left.\Gamma^{(1)}\right|_{E'-\mathrm{linear}} = -\mathfrak{A}\int dx\,[K^{-1}]_{EE}\sum_{n>1}\frac{\nu_n\mu^{(n-1)\epsilon}}{(n-2)!}E^{(n-2)}\Delta E' \tag{26}$$

where

$$[K^{-1}]_{EE} = \iint\frac{d\omega\,d\mathbf{k}}{(2\pi)^{d+1}}\frac{D_f(\omega,k)}{\omega^2 + [\mathfrak{A}k^2\mathcal{V}]^2},\quad \mathcal{V} \equiv \sum_{n\geq 1}\frac{\nu_n\mu^{(n-1)\epsilon}}{(n-1)!}E^{(n-1)}. \tag{27}$$

Integrating (27) over the frequency variable ω, viz.,

$$[K^{-1}]_{EE} = \int\frac{d\mathbf{k}}{(2\pi)^d}\frac{k^{-d-2\epsilon}}{\varrho^2(\mu/k)^{4\kappa} + \mathcal{V}^2}\left[1 + \frac{\varrho(\mu/k)^{2\kappa}}{\mathcal{V}}\right], \tag{28}$$

and expanding the result in powers of ϱ^2, we obtain [14], viz.,

$$[K^{-1}]_{EE} = -\frac{S_d}{2\pi^d}\frac{m^{-2\epsilon}}{\mathcal{V}^2}\sum_{\ell=0}^\infty(-1)^\ell\left[\frac{\varrho(\mu/m)^{2\kappa}}{\mathcal{V}}\right]^{2\ell}\left(\frac{1}{2\epsilon+4\kappa\ell} + \frac{1}{\mathcal{V}}\frac{\varrho(\mu/m)^{2\kappa}}{2\epsilon+2\kappa(2\ell+1)}\right) \tag{29}$$

where $S_d \equiv 2\pi^{d/2}/\Gamma(d/2)$ is the surface area of a unit sphere in $d-$dimensional space. Substituting the result (29) back into (26), we arrive at the following expression for the one-loop order contributions [14]:

$$\left.\Gamma^{(1)}\right|_{E'-\mathrm{linear}} \simeq \frac{\mathfrak{A}C_d}{m^{2\epsilon}}\sum_{\ell=0}^\infty(-1)^\ell\left[\varrho\left(\frac{\mu}{m}\right)^{2\kappa}\right]^{2\ell}\left(\frac{\mathcal{V}'}{\mathcal{V}^{2\ell+2}}\frac{1}{2\epsilon+4\kappa\ell} + \frac{\mathcal{V}'}{\mathcal{V}^{2\ell+3}}\frac{\varrho(\mu/m)^{2\kappa}}{2\epsilon+2\kappa(2\ell+1)}\right)\Delta E', \tag{30}$$

where $\mathcal{V}'$ is the derivative of series $\mathcal{V}$ (27) with respect to E. The quotients of series, $\mathcal{V}'/\mathcal{V}^{2\ell+2}$ and $\mathcal{V}'/\mathcal{V}^{2\ell+3}$, in (30). can be expressed in the form of the following double expansions [14], viz.,

$$\frac{V'(E)}{V^{2\ell+2}(E)} = \sum_{n=0}^\infty\sum_{m=0}^n\mu^{\epsilon(n+1)}\frac{X_{mn}\ell^m}{n!}E^n,\quad \frac{V'(E)}{V^{2\ell+3}(E)} = \sum_{n=0}^\infty\sum_{m=0}^n\mu^{\epsilon(n+1)}\frac{Y_{mn}\ell^m}{n!}E^n, \tag{31}$$

where X_{mn} and Y_{mn} are the polynomials of the variables (ν_k/ν_1), $k \leq n$ that can be calculated using (31) as the generating functions. The first three polynomials are as follows:

$$X_{00} = \frac{\nu_2}{\nu_1},\quad X_{01} = \frac{\nu_3}{\nu_1} - \frac{2\nu_2^2}{\nu_1^2},\quad X_{02} = \frac{1}{2}\frac{\nu_4}{\nu_1} - \frac{3\nu_3\nu_2}{\nu_1^2} + \frac{3\nu_2^3}{\nu_1^3}. \tag{32}$$

$$Y_{00} = \frac{v_2}{v_1}, \quad Y_{01} = -3\frac{v_2{}^2}{v_1{}^2} + \frac{v_3}{v_1}, \quad Y_{02} = \frac{1}{2}\frac{v_4}{v_1} + \frac{6v_2{}^3}{v_1{}^3} - \frac{9}{2}\frac{v_2 v_3}{v_1{}^2}. \tag{33}$$

From (30) and (31), in the minimum subtraction scheme, in the one-loop order, for the renormalization constants $Z_n = 1 - \Gamma^{(1)}\big|_{E'-\text{linear}}$, we obtain the required result (21). $\square$

6. RG-Equations for the ASM

The requirement of eliminating the divergences from the Feynman diagrams of perturbation expansion does not determine the relations between the renormalized parameters, $\mathcal{E} \equiv \{\mathfrak{A}, \varrho, v_n\}$, $n \geq 1$, and their bare values, $\mathcal{E}_0 \equiv \{\mathfrak{A}_0, \varrho_0, v_{n0}\}$, $n \geq 1$, uniquely [14]. The remaining arbitrariness is expressed by the dimensional renormalization mass μ, $d^k[\mu] = 1$, $d[\mu] = 1$. The differential operator $D_\mu \equiv \mu \partial/\partial\mu|_{\mathcal{E}_0}$ for the fixed values of bare parameters $\mathcal{E}_0$ applied to the renormalization identity of the connected Green functions, $W_n^R = Z_E^{-n} W_n$, yields the basic RG equation [14], viz.,

$$[D_{RG} + n\gamma_E]W_n^R(\mathcal{E}, \mu, \kappa, \epsilon) = 0, \quad \gamma_E \equiv D_\mu \log Z_E, \tag{34}$$

in which the RG-differential operator is defined as follows [14]:

$$D_{RG} \equiv \mu \frac{\partial}{\partial\mu}\bigg|_{\mathcal{E}_0} + \sum_{\mathcal{E}=\{\mathfrak{A},\varrho,v_n\}} \mu \frac{\partial\mathcal{E}}{\partial\mu}\bigg|_{\mathcal{E}_0} \frac{\partial}{\partial\mathcal{E}} \tag{35}$$

with summation over all renormalized parameters $\mathcal{E}$. The coefficients $D_\mu\mathcal{E}$ in the RG-differential operator (35) known as $\beta-$functions [14], viz.,

$$\beta_\varrho \equiv D_\mu\varrho, \quad \beta_n \equiv \widetilde{D}_\mu v_n, \tag{36}$$

do not have poles neither in κ nor in ϵ. The $\gamma-$functions, γ_E (34) and $\gamma_\mathcal{E} \equiv D_\mu \log Z_\mathcal{E}$ are also the analytic functions in κ and ϵ. As $Z_E = Z_\mathfrak{A}$, $Z_{E'} = Z_\varrho = Z_\mathfrak{A}^{-1}$, $Z_n \equiv Z_E^n Z_{v_n} = Z_\mathfrak{A}^n Z_{v_n}$, it follows that there are the following relations between the $\beta-$functions and $\gamma-$function [14], viz.,

$$\begin{aligned} \beta_\varrho &= \varrho[-2\kappa + \gamma_\mathfrak{A}], \quad \beta_n = v_n[-(n-1)\epsilon - \gamma_{v_n}], \\ \gamma_E &= -\gamma_{E'} = \gamma_\mathfrak{A}, \qquad\qquad \gamma_{v_n} = \gamma_n - \gamma_\mathfrak{A}, \end{aligned} \tag{37}$$

and therefore, in the one-loop approximation, the RG-differential operator takes the following form convenient for calculations:

$$\widetilde{D}_\mu\bigg|_{1-\text{loop}} \simeq -2\kappa\varrho\partial_\varrho - \epsilon \sum_{n=1}^{\infty}(n-1)v_n\partial_{v_n}. \tag{38}$$

Applying the RG-differential operator (38) to the general expression of renormalization constants given by (21), we obtain the following formula for the $\gamma-$functions [14]:

$$\gamma_n = \frac{a}{v_n}\sum_{\ell=0}^{\infty}(-1)^\ell \varrho^{2\ell} \sum_{m=0}^{n}(X_{mn} + \varrho Y_{mn})\ell^m = \frac{a}{v_n}\sum_{m=0}^{n}\frac{(X_{mn} + \varrho Y_{mn})P_m(\varrho^2)}{(1+\varrho^2)^{m+1}}, \quad n \in \mathbb{N}, \tag{39}$$

where $a \equiv 1/(2^{d-1}\pi^{d/2}\Gamma(d/2))$, and the first few polynomials $P_m(x)$ are: $P_0 = 1$, $P_1 = -x$, $P_2 = x(x-1)$, $P_3 = -x(x^2 - 4x + 1)$, $P_4 = x(x^3 - 11x^2 + 11x - 1)$, $P_5 = -x(x^4 - 26x^3 + 66x^2 - 26x + 1)$, $P_6 = x(x-1)(x^4 - 56x^3 + 246x^2 - 56x + 1)$, etc. Consequently, following [14], we obtain

$$\beta_n = v_n\left[-(n-1)\epsilon - \frac{a}{v_n}\sum_{m=0}^{n}\frac{(X_{mn} + \varrho Y_{mn})P_m(\varrho^2)}{(1+\varrho^2)^{m+1}}\right]. \tag{40}$$

Moreover, as $\gamma_{\mathfrak{A}} = a(X_{00} + \varrho Y_{00})(1 + \varrho^2)^{-1}$ and $X_{00} = Y_{00} = \nu_2/\nu_1$ [14], we obtain

$$\gamma_{\mathfrak{A}} = a\frac{\nu_2}{\nu_1}\frac{1+\varrho}{1+\varrho^2}, \quad \beta_\varrho = \varrho\left[-2\kappa + a\frac{\nu_2}{\nu_1}\frac{1+\varrho}{1+\varrho^2}\right]. \tag{41}$$

The zeros of $\beta-$functions correspond to the fixed points of an RG-Equation [12–14].

7. Plane of Fixed Points in the ASM

Possible regimes of critical scaling in a renormalizable model are associated with the IR-stable fixed points $\{\varrho_*, \nu_{n*}\}$ of the corresponding differential RG equation [13,54], such that

$$\beta_\varrho(\varrho_*, \nu_{n*}) = \beta_n(\varrho_*, \nu_{n*}) = 0, \tag{42}$$

and the Jacobian matrix $J_{ik} = \partial\beta_i/\partial\nu_k$ is positively defined, i.e., when the real parts of all its eigenvalues are positive, for small $\kappa > 0$, $\epsilon > \kappa$, and $0 < \varrho < 1$. It then follows from the explicit expressions (40) and (41) that the two parameters, ν_{1*} and ν_{2*}, can be chosen to be arbitrary, and then all other 'coordinates' of the fixed points, ϱ_* and ν_{k*}, $k > 2$, are directly found from the Equation (42) [14], e.g.,

$$\varrho_{*1} = 0, \quad \varrho_{*2,3} = \frac{a}{4\kappa}\left(\frac{\nu_{2*}}{\nu_{1*}} \pm i\sqrt{\left(\frac{\nu_{2*}}{\nu_{1*}} - \frac{4\kappa}{a}\right)^2 + 2\left(\frac{\nu_{2*}}{\nu_{1*}}\right)^2}\right), \tag{43}$$

and furthermore

$$
\begin{aligned}
\nu_{3*} &= \frac{\nu_{2*}^2}{\nu_{1*}}\frac{2+3\varrho_*^2+\varrho_*^3}{(1+\varrho_*^2)(1+\varrho_*)}, \\
\nu_{4*} &= -\frac{\epsilon}{\kappa}\nu_{1*}^2 + \frac{1}{2}\frac{\nu_{2*}^3}{\nu_{1*}^2}\frac{5\varrho_*^6+11*\varrho_*^5+15*\varrho_*^4+43\varrho_*^3+28\varrho_*^2+36\varrho_*+18}{(1+\varrho_*^2)^2(1+\varrho_*)^2}, \text{ etc.}
\end{aligned}
\tag{44}
$$

Therefore, the RG-Equation (34) possesses a two-dimensional plane of fixed points spanned with the parameters ν_{1*} and ν_{2*} in an infinite dimensional space of coupling constants $\{\varrho, \nu_k\}$ [14].

The detailed analysis of the IR-stability of fixed points on the $\{\nu_{1*}, \nu_{2*}\}$-plane in an infinite dimensional space seems an impossible task. Below, we only discuss the important special cases of the model, such as the "white noise" and "frozen" configurations of stochastic forces fostering energy pumping into the system.

1. If there were *no time-scale separation* in the ASM (zero correlation time $t_c(k) = 0$ for all wave numbers k), i.e., for the "white noise" model of energy injection uncorrelated in space and time, viz.,

    $$\langle f(x)f(x')\rangle = 2\Gamma\delta^d(\mathbf{r} - \mathbf{r}')\delta(t - t'), \tag{45}$$

    we have $\varrho_* \to \infty$, and $\kappa = 0$, so that all $J_{nm} \approx -(n-1)\epsilon\delta_{mn} < 0$ where δ_{mn} is the Kronecker symbol. Therefore, there are *no IR-stable fixed points* in the ASM. The time scale separation is important for the existence of critical scaling regimes in the ASM.

2. In the opposite case of the "frozen" configuration of stochastic force, the first, trivial solution $\varrho_* = 0$ comes into play, and therefore $J_{nm} = -(n-1)\epsilon\delta_{nm} < 0$. Therefore, there are *no IR-stable fixed points* in the ASM in this case.

In general, as the Jacobian matrix J_{nm} has a block-triangular form, its eigenvalues coincide with the matrix diagonal entries [14], viz.,

$$J_{nn} = (1-n)\epsilon + a\sum_{m=0}^{n}\frac{\partial_{\nu_n}(X_{mn} + \varrho Y_{mn})P_m(\varrho_*^2)}{(1+\varrho_*^2)^{m+1}}. \tag{46}$$

These eigenvalues are positive, e.g.,

$$J_{00} = -a\varrho_* \frac{\nu_{2*}}{\nu_{1*}} \frac{\varrho_*^2 + 2\varrho_* - 1}{(1+\varrho_*^2)^2} > 0, \quad J_{11} = -\frac{2a}{\nu_{1*}^2(1+\varrho_*^2)}\left(\nu_{3*} - \frac{\nu_{2*}^2}{\nu_{1*}} \frac{5+\varrho_*^2}{1+\varrho_*^2}\right) > 0, \text{ etc. } \quad (47)$$

whenever

$$\frac{\varrho_*^3 + 3\varrho_*^2 - 2 - 4\varrho_*}{(1+\varrho_*)(1+\varrho_*^2)} < 0, \quad \frac{2\varrho_*^2 - 3 - 5\varrho_*}{(1+\varrho_*)(1+\varrho_*^2)} < 0, \text{ etc.} \quad (48)$$

Although both inequalities in (48) are always true for $0 < \varrho_* < 1$, others may not be. The IR-stability domains of the fixed points in the ASM are ultimately defined by the existence and exact location of the roots in the interval $0 < \varrho_* < 1$ for an infinite number of polynomials in ϱ_* that can split the $\{\nu_{1*}, \nu_{2*}\}$-plane of fixed points into a number of IR-stable and unstable regions [14]. It is also important to note that, even if the IR-stable fixed points of an RG equation exist in a model with multiple coupling-constants, the actual RG-trajectory of the system starting from the particular initial conditions may not achieve any of them. In our case, the RG-trajectory evolves from the bare parameters $\{\varrho_0, \nu_{k0}\}$ in the infinite dimensional space of coupling constants $\{\varrho, \nu_k\}$, none of which can be neglected [14]. The RG-trajectory can leave the stability domain by breaking the scaling behavior that is often interpreted in the critical phenomena theory as the first-order phase transition [11–14].

8. On the Critical Scaling in the ASM

Nevertheless, let us suppose that there exists an IR-stable domain in the $\{\nu_{1*}, \nu_{2*}\}$-plane of fixed points in the ASM. Then, the leading terms of the long-time large-scale asymptotic of the renormalized connected Green functions W_n^R satisfy the RG-equation (34) at the IR-stable fixed points ϱ_*, ν_{n*}, $n > 2$. It is worth mentioning that the corresponding value of the anomalous dimension $\gamma_{\mathfrak{A}*}$ defined in (41) is exact, requiring no further corrections neither in ϵ, nor in κ, viz.,

$$\gamma_{\mathfrak{A}*} = 2\kappa, \quad (49)$$

and, therefore, the critical dimensions of all quantities under the scaling of $x \equiv t$, $\mathbf{r}$ at the fixed values of μ, $\mathfrak{A}$, ϱ and ν_n can be readily calculated. The equation of critical scaling for the renormalized connected Green functions W_n^R comprising n_E renormalized fields E and $n_{E'}$ renormalized fields E' takes the following form [14]:

$$[-D_x + \Delta[t]D_t - n_E\Delta_E - n_{E'}\Delta_{E'}]W_n^R = 0 \quad (50)$$

where the coefficients and the critical dimensions of time and fields are given by

$$\Delta[t] = -\Delta[\omega] = -2 + \gamma_{\mathfrak{A}*} = -2 + 2\kappa, \quad \Delta[E] = 2\kappa - \epsilon, \quad \Delta[E'] = d + \epsilon - 2\kappa. \quad (51)$$

The critical dimension of time $\Delta[t] = -2 + 2\kappa$ corresponds to the dimension of the reciprocal correlation time $t_c(k) \propto k^{-2+2\kappa}$ in the power injection model (7). The critical dimensions of fields E and E' for the different assumptions on energy injection in the ASM are given following [14] in Table 2.

In Section 2, we discussed that, for the random force *uncorrelated in space*, $D_F(k) \propto$ Const, and therefore, the 'real' value of the expansion parameter ϵ should satisfy $6 - d - 2\epsilon_{\text{real}} - 2\kappa = 0$, or $\epsilon_{\text{real}} = 3 - \kappa - d/2$. Under the "white noise" assumption, it should be considered that $\epsilon_{\text{real}} = 1 - d/2 + \kappa$, although the corresponding fixed points of RG-transformation are not IR-stable for the lack of time-scale separation between the energy pumping and relaxation processes. Finally, $\epsilon_{\text{real}} = 4 - d$, for the "frozen" configuration of random force that is also not IR-stable.

Table 2. The critical dimensions of the fields E and E' for the different assumptions on energy injection in the ASM [14].

Assumption on Random Force	ϵ_{real}	$\Delta[E]$	$\Delta[E']$	IR-Stability
Uncorrelated in space	$3 - \kappa - d/2$	$d/2 + 3(\kappa - 1)$	$d/2 + 3(1 - \kappa)$	Domain-wise
"White noise"	$1 - d/2 + \kappa$	$d/2 + \kappa - 1$	$d/2 + 1 - \kappa$	No
"Frozen" configuration	$4 - d$	$2\kappa - 4 + d$	$4 - 2\kappa$	No

For example, similarly to the famous Kolmogorov $-5/3$-law for the energy spectrum in fully developed turbulence, we can say that the leading long-term, large-scale asymptotic renormalized Green function $< EE >^R$ for the ASM acquires the following scaling representation in Fourier space (k-representation) [13,54], viz.,

$$\langle E(-\mathbf{k}, 0)E(\mathbf{k}, t)\rangle \simeq_{k \to 0} k^{2\Delta[E] - d + \Delta[t]} \mathcal{H}\left(tk^{\Delta[t]}, kL, k/\mu, \mathfrak{A}\varrho k^{2 - 2\kappa}, \{\nu_n\}_{n=1}^\infty\right) \qquad (52)$$

where $\Delta[E]$ and $\Delta[t]$ are the critical dimensions of energy E and time t, and $\mathcal{H}$ is a scaling function of the dimensionless arguments that is not determined by the RG-equation [13]. The critical dimension of $< EE >^R$ for the different assumptions on energy injection enlisted in Table 2 is given by

$$\Delta\left[< EE >^R\right] = 2\Delta[E] - d + \Delta[t] = \begin{cases} -8 + 8\kappa, & \text{Uncorrelated in space,} \\ -4 + 4\kappa, & \text{White noise (IR} - \text{unstable),} \\ d + 6\kappa - 10, & \text{Frozen (IR} - \text{unstable).} \end{cases} \qquad (53)$$

For the static Green function,

$$< EE >_{\text{st}}^R (k) = \frac{1}{2\pi} \int d\omega \, < EE >^R (\omega, k), \qquad (54)$$

the following long-term, large-scale asymptotic is obtained:

$$\langle E(-\mathbf{k})E(\mathbf{k})\rangle_{st} \propto_{k \to 0} k^{2\Delta[E] - d}, \qquad (55)$$

so that

$$\Delta\left[< EE >_{st}^R\right] = 2\Delta[E] - d = \begin{cases} -6 + 6\kappa, & \text{Uncorrelated in space,} \\ -2 + 2\kappa, & \text{White noise (IR} - \text{unstable),} \\ d + 4\kappa - 8, & \text{Frozen (IR} - \text{unstable).} \end{cases} \qquad (56)$$

The response function $\langle E'(-\mathbf{k}, 0)E(\mathbf{k}, t)\rangle$ evaluates the average size of the relaxation process (an avalanche) arisen in the system as a reaction for a point-wise perturbation occurring at time $t' = 0$. For the long-term, large-scale asymptotic of $\langle E'(-\mathbf{k}, 0)E(\mathbf{k}, t)\rangle$, we obtain:

$$\langle E'(-\mathbf{k}, 0)E(\mathbf{k}, t)\rangle \propto_{k \to 0} k^{\Delta[E'] + \Delta[E] - d + \Delta[t]} = k^{\Delta[t]} = k^{-2 + 2\kappa}, \qquad (57)$$

uniformly for all critical regimes [14]. Finally, we calculate the asymptotic squared effective radius of an avalanche at time $t > 0$ started at $t' = 0$ at the origin $\mathbf{x} = 0$ [14], viz.,

$$R^2 = \int d\mathbf{x} \, \mathbf{x}^2 \langle E(\mathbf{x}, t)E'(\mathbf{0}, 0)\rangle. \qquad (58)$$

As $\Delta[R] = -1$ by convention, and $\Delta[dR^2/dt] = -2 - \Delta[t]$, we obtain the following equation for the avalanche size spectrum [14]:

$$\frac{dR^2}{dt} \propto R^{2\kappa} \qquad (59)$$

that is similar to the well-known Richardson "four-thirds" phenomenological law for the diffusion of passive admixtures in an ambient turbulent flow [50–52], viz.

$$\frac{dR^2}{dt} \simeq R^{4/3}. \tag{60}$$

The equation $d\mathcal{A}/dT = K\mathcal{A}^{\kappa}$ with some constant K for the effective area covered by an avalanche $\mathcal{A}(T) \propto R^2(T)$ as a function of a (sufficiently long) avalanche duration T corresponding to (59) has the following general solution:

$$\mathcal{A}(T) = (\mathcal{A}_0 + K(1 - \kappa)T)^{\frac{1}{1-\kappa}} \propto (1 - \kappa)T^{\frac{1}{1-\kappa}} \tag{61}$$

exhibiting a super-linear growth of the avalanche area with a duration in the correlated energy injection introducing the time-scale separation in the model, as $\kappa > 0$. For instance, $\mathcal{A}(T) \propto 3T^3$, or $R(T) \propto T^{3/2}$, for the Richardson law of turbulent transport (60) where $\kappa = 2/3$. The same exponent value is observed for the first-return time statistics of random walks in the excursions of a time series above some given (arbitrary) threshold [58] and for an Ornstein–Uhlenbeck process [59]. Under the "white noise" assumption, $\kappa = 0$, which corresponds to a linear size–time relation, $R(T) \propto T$, that is typical for the tent-like shape avalanches observed in crack propagation experiments [60] and for the Barkhausen noise in amorphous ferromagnetic films [61].

Finally, in many different contexts in applied science and engineering, there are avalanche phenomena of widely varied duration and sizes. Such avalanches frequently have probability distributions with a "fat-tail" that fits well with a power-law distribution (61) for different values of κ. They include but are not limited to the vortices of superconductors [62], Barkhaussen noise [63], X-ray flares [25], earthquakes [17], rainfall [64], and failures on electrical power grids [65]. The collection of observed exponents, $R(T) \propto T^{\kappa}$, where $\kappa \simeq 2$ is documented by empirical means, aligns with the well-known Galton–Watson branching processes [66,67] and corresponds to $\kappa = 1/2$ in the model that seems to be ubiquitous in propagation dynamics in real-world networking systems [68,69].

9. Discussion and Conclusions

We have studied long-term and large-scale asymptotic behavior in the ASM model of SOC introduced by Bak, Tang, and Wiesenfeld [1]. This model has been extremely stimulating, playing a fundamental role in SOC that is somewhat similar to the role played by the famous Ising model of ferromagnetism in statistical mechanics [9].

In our work, the stochastic problem corresponding to the ASM model is considered in the bulk, far from boundaries, and energy dissipation occurs at every point. We used the field theory formulation of the stochastic problem and apply the RG-technique developed in quantum field theory to investigate the critical scaling in the ASM, with an infinite number of coupling constants. Our major result is the proof of the multiplicative UV-renormalization of the ASM and the calculation of an infinite number of renormalization constants (required for the simultaneous subtraction of all UV-singularities in perturbation theory) in the one-loop order. We found the critical exponents for all correlation functions of energy field E, as well as all response functions, both in dynamics and statics, for the different assumptions on the energy injection. We have proven that the simplest "white noise" assumption on the covariance of stochastic force pumping energy into the model does not correspond to the stable long-time, large-scale asymptotic behavior due to lack of time-scale separation between the slow energy injection and fast avalanche relaxation processes. The random force covariance characterized by the correlation time $t_c(k) \propto k^{-2+2\kappa}$ scales at a wave number k with some phenomenological parameter $2\kappa > 0$ seems more realistic, as restoring the time-scale separation that appears in the original models [1], demonstrating the self-organized critical behavior.

The RG-transformation of ASM takes place in an infinitely dimensional space of coupling constants corresponding to the competing terms of the power series expansion

reflecting a threshold nature of relaxation processes. It is worth mentioning that, despite the values of coupling constants are small, none of these expansion terms can be omitted from consideration, as their contributions are equally important for the analysis of long-term, large-scale behavior of the model. Nevertheless, the first two coupling constants play an important role among others, thus featuring a *two-dimensional plane* of fixed points of the RG-transformation. It is important to mention that manifolds of fixed points of the RG transformation have already been observed in the study of a self-organized critical system. Namely, a *curve* of fixed points has recently been discovered [47] in a strongly anisotropic continuous (coarse-grained) model coupled to an isotropic random fluid environment introduced in [70,71]. If the IR-stable domains in the plane of fixed points exist, the long-term and large-scale asymptotic behavior is characterized by critical scaling with the critical dimensions of the energy field E given in Table 2 for the different models of energy injection specified by the index $2\kappa > 0$. It is important to note that our results concerning the critical dimensions enlisted in Table 2 are "exact" in the sense that they do not require further corrections in terms of the model parameters ϵ and κ. However, the IR-stability domains on the plane of fixed points of the RG transformation indeed depend on the values of model parameters. As we have shown, some regimes that arise at certain values of model parameters may be not IR-stable, although we have also formally calculated critical dimensions for them.

Further research is needed to focus on the possible modifications of critical behavior close to the absorbing boundary. For example, Equation (5) can be considered in a half-space $x > 0$, with a pseudo-random force acting at the boundary $x = 0$ to ensure the dissipation of energy, viz., $f|_{x=0} < 0$. The semi-infinite geometry of the modified model would change the transfer of energy along the boundary that effectively decouples the critical behavior in the bulk and at the boundary. The lattice topology would also play an important role, as if the coordination number q of a lattice site is large, the toppled amount of energy dissipated at the open boundary would be much smaller than that transferred to other neighbors, so that the perturbation of the behavior risen by the force $f|_{x=0}$ close to the boundary would not propagate into the bulk of lattice. Otherwise, a critical slope can appear at the boundary if the energy dissipation dominates the process of the energy transfer to the neighboring sites.

Institutional Review Board Statement: Not applicable.

Data Availability Statement: Data are contained within the article.

Conflicts of Interest: The author declares no conflicts of interest.

Abbreviations

The following abbreviations are used in this manuscript:

ACM	Abelian sandpile model
IR	Infra-red (momentum scale)
RG	Renormalization group
SOC	Self-organized criticality
UV	Ultra-violet (momentum scale)

References

1. Bak, P.; Tang, C.; Wiesenfeld, K. Self-organized criticality: An explanation of $1/f$ noise. *Phys. Rev. Lett.* **1987**, *59*, 381–384. [CrossRef] [PubMed]
2. Dhar, D. Self-organized Critical State of Sandpile Automaton Models. *Phys. Rev. Lett.* **1990**, *64*, 1613–1616. [CrossRef] [PubMed]
3. Zhang, Y.-C. Scaling theory of self-organized criticality *Phys. Rev. Lett.* **1989**, *63*, 470. [CrossRef] [PubMed]
4. Bak, P. *How Nature Works*; Springer: Berlin/Heidelberg, Germany, 1996.

5.   Newman, M.E.J.; Sneppen, K. Avalanches, scaling, and coherent noise. *Phys. Rev. E* **1996**, *54*, 6226. [CrossRef] [PubMed]
6.   Sneppen, K.; Newman, M.E.J. Coherent noise, scale invariance and intermittency in large systems. *Phys. D* **1997**, *110*, 209. [CrossRef]
7.   Eyink, G.L.; Hussein, A. The breakdown of Alfven's theorem in ideal plasma flows: Necessary conditions and physical conjectures. *Phys. D* **2006**, *223*, 82. [CrossRef]
8.   Jensen, H.J. *Self-Organized Criticality: Emergent Complex Behavior in Physical and Biological Systems*; Cambridge Lecture Notes in Physics 10; Cambridge University Press: Cambridge, UK, 1998.
9.   Watkins, N.W.; Pruessner, G.; Chapman, S.C.; Crosby, Jensen, H.J. 25 Years of Self-organized Criticality: Concepts and Controversies. *Space Sci. Rev.* **2016**, *198*, 3–44. [CrossRef]
10. Bak P.; Paczuski M. Complexity, contingency, and criticality. *Proc. Natl. Acad. Sci. USA* **1995**, *92*, 6689–6696. [CrossRef]
11. Ma, S.K. *Modern Theory of Critical Phenomena*; Reading, B., Ed.; Routledge: Londin, UK, 1976.
12. Zinn-Justin, J. *Quantum Field Theory and Critical Phenomena*; Clarendon: Oxford, UK, 1990.
13. Vasiliev, A.N. *The Field Theoretic Renormalization Group in Critical Behaviour Theory and Stochastic Dynamics*; Chapman & Hall/CRC: Boca Raton, FL, USA, 2004.
14. Volchenkov, D. Renormalization group and instantons in stochastic nonlinear dynamics: From self-organized criticality to thermonuclear reactors. *Eur. Phys. J.-Spec. Top.* **2009**, *170*, 1–142 . [CrossRef]
15. Turcotte, D.L. Self-organized criticality. *Rep. Prog. Phys.* **1999**, *62*, 1377. [CrossRef]
16. Chialvo, D.R. Emergent complex neural dynamics. *Nat. Phys.* **2010**, *6*, 744–750. [CrossRef]
17. Bak, P.; Christensen, K.; Danon, L.; Scanlon, T. Unified Scaling Law for Earthquakes. *Phys. Rev. Lett.* **2002**, *88*, 178501. [CrossRef] [PubMed]
18. Turcotte, D.L. Seismicity and self-organized criticality. *Phys. Earth Planet. Inter.* **1999**, *111*, 275–293. [CrossRef]
19. Sheinman, M.; Sharma, A.; Alvarado, J.; Koenderink, G.H.; MacKintosh, F.C. Anomalous Discontinuity at the Percolation Critical Point of Active Gels. *Nat. Phys.* **2013**, *9*, 591. [CrossRef]
20. Beggs, J.M.; Plenz, D. Neuronal avalanches in neocortical circuits. *J. Neurosci.* **2003**, *23*, 11167–11177. [CrossRef]
21. Hesse, J.; Gross, T. Self-organized criticality as a fundamental property of neural systems. *Front. Syst. Neurosci.* **2014**, *8*, 166. [CrossRef]
22. Meisel, C.; Storch, A.; Hallmeyer-Elgner, S.; Bullmore, E.; Gross, T. Failure of adaptive self-organized criticality during epileptic seizure attacks. *PLoS Comput. Biol.* **2012**, *8*, e1002312. [CrossRef]
23. Plenz, D.; Ribeiro, T.L.; Miller, S.R.; Kells, P.A.; Vakili, A.; Capek, E.L. Self-Organized Criticality in the Brain. *Front. Phys.* **2021**, *9*, 639389. [CrossRef]
24. Audard, M.; Güdel, M.; Drake, J.J.; Kashyap, V.L. Extreme-Ultraviolet Flare Activity in Late-Type Stars. *Astrophys. J.* **2000**, *541*, 396. [CrossRef]
25. Wang, F.; Dai, Z. Self-organized criticality in X-ray flares of gamma-ray-burst afterglows. *Nat. Phys.* **2013**, *9*, 465–467. [CrossRef]
26. McKenzie, D.; Kennedy, M. Power laws reveal phase transitions in landscape controls of fire regimes. *Nat. Commun.* **2012**, *3*, 726. [CrossRef] [PubMed]
27. Hantson, S.; Scheffer, M.; Pueyo, S.; Xu, C.; van Nes, E.H.; Holmgren, M.; Mendelsohn, J. Rare, Intense, Big fires dominate the global tropics under drier conditions. *Sci. Rep.* **2017**, *7*, 14374. [CrossRef] [PubMed]
28. Li, Z. Self-organized criticality dynamic of forest fire model. *Indian J. Phys.* **2023**, *97*, 1959–1964. [CrossRef]
29. Kron, T.; Grund, T.U. Society as a Self-Organized Critical System. *Cybern. Hum. Knowing* **2009**, *16*, 65–82.
30. A cikalin, Ş.N.; Artun, E.C. The concept of self-organized criticality: The case study of the Arab uprising. In *Chaos, Complexity and Leadership 2017: Explorations of Chaos and Complexity Theory*; Springer International Publishing: Berlin/Heidelberg, Germany, 2019; Volume 5, pp. 73–85.
31. Zhukov, D. How the theory of self-organized criticality explains punctuated equilibrium in social systems. *Methodol. Innov.* **2022**, *15*, 163–177. [CrossRef]
32. Hoffmann, H.; Payton, D.W. Optimization by Self-Organized Criticality. *Sci. Rep.* **2018**, *8*, 2358. [CrossRef]
33. Ramos, R.T.; Sassi, R.B.; Piqueira, J.R.C. Self-organized criticality and the predictability of human behavior. *New Ideas Psychol.* **2011**, *29*, 38–48. [CrossRef]
34. Walter, N.; Hinterberger, T. Self-organized criticality as a framework for consciousness: A review study. *Front. Psychol.* **2022**, *13*, 911620. [CrossRef]
35. Díaz-Guilera, A. Noise and dynamics of self-organized critical phenomena. *Phys. Rev. A* **1992**, *45*, 8551. [CrossRef]
36. Collins, J. *Renormalization: An Introduction to Renormalization, the Renormalization Group, and the Operator -Product Expansion*; Cambridge University Press: Cambridge, UK, 1992.
37. Pietronero, L.; Vespignani, A.; Zapperi, S. Renormalization scheme for self-organized criticality in sandpile models. *Phys. Rev. Lett.* **1994**, *72*, 1690. [CrossRef]
38. Zapperi, S.; Vespignani, A.; Pietronero, L. Real Space Renormalization Group for Self Organized Criticality in Sandpile Models. *MRS Online Proc. Libr.* **1994**, *367*, 67–71. [CrossRef]
39. Díaz-Guilera, A. Dynamic renormalization group approach to self-organized critical phenomena. *Europhys. Lett.* **1994**, *26*, 177. [CrossRef]
40. Hasty, J.M. *A Renormalization Group Study of Self-Organized Criticality*; Georgia Institute of Technology: Atlanta, GA, USA, 1997.

41. Corral, A.; Díaz-Guilera, A. Symmetries and fixed point stability of stochastic differential equations modeling self-organized criticality. *Phys. Rev. E* **1997**, *55*, 2434. [CrossRef]

42. Giacometti, A.; Díaz-Guilera, A. Dynamical properties of the Zhang model of self-organized criticality. *Phys. Rev. E* **1998**, *58*, 247. [CrossRef]

43. Chang, T. Self-organized criticality, multi-fractal spectra, sporadic localized reconnections and intermittent turbulence in the magnetotail. *Phys. Plasmas* **1999**, *6*, 4137–4145. [CrossRef]

44. Antonov, N.V.; Kakin, P.I. Effects of random environment on a self-organized critical system: Renormalization group analysis of a continuous model. In *EPJ Web of Conferences*; EDP Sciences: Les Ulis, France, 2016; Volume 108, p. 02009.

45. Antonov, N.V.; Gulitskiy, N.M.; Kakin, P.I.; Serov, V.D. Effects of turbulent environment and random noise on self-organized critical behavior: Universality versus nonuniversality. *Phys. Rev. E* **2021**, *103*, 042106. [CrossRef]

46. Antonov, N.V.; Gulitskiy, N.M.; Kakin, P.I.; Semeikin, M.N. Dimensional transmutation and nonconventional scaling behavior in a model of self-organized criticality. *Int. J. Mod. Phys. A* **2022**, *37*, 2240022. [CrossRef]

47. Antonov, N.V.; Kakin, P.I.; Lebedev, N.M.; Luchin, A.Y. Renormalization group analysis of a self-organized critical system: Intrinsic anisotropy vs. random environment. *J. Phys. Math. Theor.* **2023**, *56*, 375002. [CrossRef]

48. Antonov, N.V.; Vasil'ev A.N. The quantum-field renormalization group in the problem of a growing phase boundary. *J. Exp. Theor. Phys.* **1995**, *81*, 485–489.

49. Antonov, N.V. The renormalization group in the problem of turbulent convection of a passive scalar impurity with nonlinear diffusion. *J. Exp. Theor. Phys.* **1997**, *85*, 898–906. [CrossRef]

50. Monin, A.S.; Yaglom, A.M. *Statistical Fluid Mechanics*; Volumes 1 and 2 ; MIT Press: Cambridge, MA, USA, 1971 .

51. Nakao, H.; Imamura, T. Mechanism in Leading to Richardson's Four-Thirds Law. *J. Phys. Soc. Jpn.* **1992**, *61*, 2772–2778. [CrossRef]

52. Dubkov, A.A.; Spagnolo, B.; Uchaikin, V.V. Lévy Flight Superdiffusion: An Introduction. *Int. J. Bifurc. Chaos* **2008**, *18*, 2649–2672. [CrossRef]

53. Pietronero, L.; Tartaglia, P. ; Zhang, Y.-C. Theoretical studies of self-organized criticality. *Phys. Stat. Mech. Its Appl.* **1991**, *173*, 22–44. [CrossRef]

54. Adzhemyan, L.T.; Antonov, N.V.; Vasil'ev, A.N. *The Field Theoretic Renormalization Group in Fully Developed Turbulence*; Gordon and Breach: London, UK, 1999.

55. Martin, P.C.; Siggia, E.D.; Rose, H.A. Statistical Dynamics of Classical Systems. *Phys. Rev. A* **1973**,*8*, 423. [CrossRef]

56. de Dominicis, C.; Peliti, L. Field-theory renormalization and critical dynamics above T_c: Helium, antiferromagnets, and liquid-gas systems. *Phys. Rev. B* **1978**, *18*, 353. [CrossRef]

57. Wyld, H.W. Formulation of the theory of turbulence in an incompressible fluid. *Ann. Phys.* **1961**, *14*, 143. [CrossRef]

58. di Santo, S.; Villegas, P.; Burioni, R.; Muñoz, M. Simple unified view of branching process statistics: Random walks in balanced logarithmic potentials. *Phys. Rev. E* **2017**, *95*, 032115. [CrossRef]

59. Villegas, P.; di Santo, S.; Burioni, R.; Muñoz, M.A. Time-series thresholding and the definition of avalanche size. *Phys. Rev. E* **2019**, *100*, 012133. [CrossRef]

60. Laurson, L.; Illa, X.; Santucci, S.; Tallakstad, K.T.; Maloy, K.J.; Alava, M.J. Evolution of the average avalanche shape with the universality class. *Nat. Commun.* **2013**, *4*, 2927. [CrossRef]

61. Papanikolaou, S.; Bohn, F.; Sommer, R.L.; Durin, G.; Zapperi, S.; Sethna, J.P. Universality beyond power laws and the average avalanche shape. *Nat. Phys.* **2011**, *7*, 316. [CrossRef]

62. Altshuler, E.; Johansen, T. Colloquium: Experiments in vortex avalanches. *Rev. Mod. Phys.* **2004**, *76*, 471. [CrossRef]

63. Aless, ro, B.; Beatrice, C.; Bertotti, G.; Montorsi, A. Domain-wall dynamics and Barkhausen effect in metallic ferromagnetic materials. I, Theory. *J. Appl. Phys.* **1990**, *68*, 2901.

64. Peters, O.; Hertlein, C.; Christensen, K. A Complexity View of Rainfall. *Phys. Rev. Lett.* **2001**, *88*, 018701. [CrossRef] [PubMed]

65. Kinney, R.; Crucitti, P.; Albert, R.; Latora, V. Modeling cascading failures in the North American power grid. *Eur. Phys. J. B-Condens. Matter Complex Syst.* **2005**, *46*, 101. [CrossRef]

66. Watson, H.W.; Galton, F. On the Probability of the Extinction of Families. *J. Anthropol. Inst. Great Br. Irel.* **1875**, *4*, 138–144. [CrossRef]

67. Liggett, T. *Interacting Particle Systems*; Springer Series: Classics in Mathematics; Springer: New York, NY, USA, 2004.

68. Binney, J.; Dowrick, N.; Fisher, A.; Newman, M. *The Theory of Critical Phenomena*; Oxford University Press: Oxford, UK, 1993.

69. Karrer, B.; Newman, M.E.; Zdeborová, L. Percolation on Sparse Networks. *Phys. Rev. Lett.* **2014**, *113*, 208702. [CrossRef]

70. Hwa, T.; Kardar, M. Dissipative transport in open systems: An investigation of self-organized criticality. *Phys. Rev. Lett.* **1989**, *62*, 1813. [CrossRef]

71. Hwa, T.; Kardar, M. Avalanches, hydrodynamics and discharge events in models of sandpiles. *Phys. Rev. A* **1992**, *45*, 7002. [CrossRef]